



# CHORUS

This is the accepted manuscript made available via CHORUS. The article has been published as:

## Cavity-Free Optical Isolators and Circulators Using a Chiral Cross-Kerr Nonlinearity

Keyu Xia, Franco Nori, and Min Xiao

Phys. Rev. Lett. **121**, 203602 — Published 14 November 2018

DOI: [10.1103/PhysRevLett.121.203602](https://doi.org/10.1103/PhysRevLett.121.203602)

# Cavity-free optical isolators and circulators using a chiral cross-Kerr nonlinearity

Keyu Xia,<sup>1,2,3,\*</sup> Franco Nori,<sup>3,4</sup> and Min Xiao<sup>1,2,5</sup>

<sup>1</sup>National Laboratory of Solid State Microstructures, College of Engineering and Applied Sciences, and School of Physics, Nanjing University, Nanjing 210093, China

<sup>2</sup>Collaborative Innovation Center of Advanced Microstructures, Nanjing University, Nanjing 210093, China

<sup>3</sup>Theoretical Quantum Physics Laboratory, RIKEN Cluster for Pioneering Research, Wako-shi, Saitama 351-0198, Japan

<sup>4</sup>Physics Department, The University of Michigan, Ann Arbor, Michigan 48109-1040, USA

<sup>5</sup>Department of Physics, University of Arkansas, Fayetteville, Arkansas 72701, USA

(Dated: October 17, 2018)

Optical nonlinearity has been widely used to try to produce optical isolators. However, this is very difficult to achieve due to dynamical reciprocity. Here, we show the use of the chiral cross-Kerr nonlinearity of atoms at room temperature to realize optical isolation, circumventing dynamical reciprocity. In our approach, the chiral cross-Kerr nonlinearity is induced by the thermal motion of N-type atoms. The resulting cross phase shift and absorption of a weak probe field are dependent on its propagation direction. This proposed optical isolator can achieve more than 30 dB of isolation ratio, with a low loss of less than 1 dB. By inserting this atomic medium in a Mach-Zehnder interferometer, we further propose a four-port optical circulator with a fidelity larger than 0.9 and an average insertion loss less than 1.6 dB. Using atomic vapor embedded in a on-chip waveguide, our method may provide chip-compatible optical isolation at the single-photon level of a probe field.

*Introduction.* — Optical isolation is highly desirable for lasers, optical information processing, and quantum networks [1, 2]. It requires optical non-reciprocity, i.e., breaking of Lorentz reciprocity [3], but is very challenging to achieve without applying magnetic fields.

Non-magnetic optical isolation is chip-compatible and therefore is in great demand for integrated optical signal processing. It has been studied via dynamically modulating material permittivity [4–7], inducing a photonic Berry phase [8–11], twisting a resonator [12], fast spinning resonator [13], or using optomechanical systems [10, 14–16]. Over the past decades, optical nonlinearity (in particular, Kerr or Kerr-like nonlinearity) has attracted intense research as a chip-compatible candidate for magnetic-free optical isolation [17–22]. Moreover, using a gain medium has also been demonstrated for optical isolation [19–21, 23, 24]. However, optical isolators with nonlinearity or gain in the medium are subject to dynamic reciprocity [25, 26]. Therefore, this kind of device is non-reciprocal only for strong signals with particular intensity, but fail to isolate weak signals. A chiral gain has been recently used to overcome this fundamental barrier in nonlinear isolators [22, 23]. However, a passive nonlinear isolator without dynamic reciprocity would be of interest. Moreover, most of the existing schemes for optical isolation require high-quality resonators or cryogenic temperature.

Instead of classical optics, quantum optics provides a tool to control photon propagation, including electromagnetically induced transparency (EIT) [27–29], optical non-reciprocity [30–32] and chirality [33–38]. Light propagating in a “moving” Bragg lattice created in atoms is subject to a “macroscopic” Doppler effect and has demonstrated non-reciprocity [39–41]. By using a chiral quantum system, optical isolation has been achieved at the single-photon level [42–45].

Optical chirality has been widely exploited to engineer spin-orbital interaction of light [33–37]. In this letter, we propose how to achieve efficient optical isolation using chi-

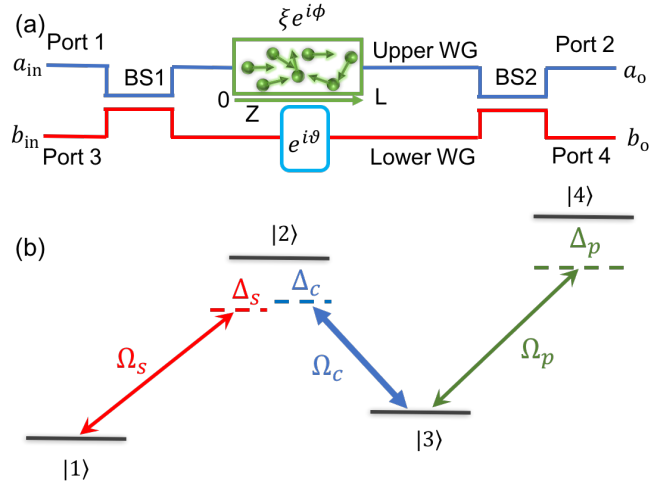


FIG. 1. (Color online) (a) Schematic diagram of our setup for optical isolator and circulator. For an optical isolator, we only consider the upper channel embedded with a cloud of N-type atoms. The photon passing through the atoms suffers a phase shift  $\phi$  and an amplitude transmission of  $\xi$ , dependent on its propagation direction. To perform an optical circulator, the lower channel is added to form a Mach-Zehnder interferometer, using beam splitters BS1 and BS2, with the upper one. In the lower branch, a phase shift  $\theta$  is used to compensate the phase shift of the backward-moving photon in the upper branch. (b) Level diagram of N-type atoms. The switching ( $\Omega_s$ ), coupling ( $\Omega_c$ ) and probe ( $\Omega_p$ ) fields couple to the transitions  $|1\rangle \leftrightarrow |2\rangle$ ,  $|3\rangle \leftrightarrow |2\rangle$  and  $|3\rangle \leftrightarrow |4\rangle$ , with detunings  $\Delta_s$ ,  $\Delta_c$ , and  $\Delta_p$ , respectively.

ral cross-Kerr (XKerr) nonlinearity induced in atoms. Due to the chirality of atomic nonlinearity, the phases and amplitudes of the forward- (right-) and backward-moving (left-moving) probe fields are very different after passing through atoms along two opposite directions. Therefore, both of optical isolator and circulator can be achieved with high isolation ratio and low insertion loss. Because the induced nonlinearity is chiral, our proposals circumvent the problem of dynamic

reciprocity, and may provide a new cavity-free route for non-linear optical isolators and circulators.

*System and model.* — Our setup is depicted in Fig. 1. We first consider a waveguide (WG) embedded with N-type atoms [46–50], see the upper waveguide in Fig. 1(a). We apply the classical switching and coupling fields to induce the phase shift  $\phi$ , and amplitude modulation  $\xi$  of the probe field. To a good approximation, we treat the waveguide as a 1D space. If the forward and backward amplitude transmissions  $\xi_f$  and  $\xi_b$  are sufficiently different after the probe field passes through the ensemble of atoms, then we can realize a two-port optical isolator. By carefully choosing the density and length of the atomic vapor and properly arranging the switching and coupling fields, we can obtain a phase shift difference,  $\Delta\phi = \phi_f - \phi_b$ , approaching  $\pi$  with high transmissions  $\xi_f$  and  $\xi_b$ . This can provide a four-port optical circulator by adding a lower waveguide to form a Mach-Zehnder interferometer (MZI).

We consider a N-type configuration using Rubidium (Rb) atoms to create the chiral XKerr nonlinearity. The state  $|2\rangle$  decays to states  $|1\rangle$  and  $|3\rangle$  with rates  $\gamma_{21}$  and  $\gamma_{23}$ , respectively. The state  $|4\rangle$  decays at a rate  $\gamma_{43}$ . The dephasing rates of both ground states  $|1\rangle$  and  $|3\rangle$  are  $\Gamma$ . For simplicity, we assume  $\gamma_{21} = \gamma_{23} = \gamma_{34} = \gamma_0$  and  $\Gamma \ll \gamma_0$ ; and set  $\gamma_0 = 2\pi \times 6$  MHz [51]. The XKerr nonlinearity can be efficiently induced between the probe and switching fields in the configuration shown in Fig. 1(b), and can be modified by the coupling laser [52]. The switching, coupling, and probe laser beams have carrier frequencies  $\omega_s$ ,  $\omega_c$ , and  $\omega_p$ , corresponding to wave vectors  $k_s$ ,  $k_c$ , and  $k_p$ , respectively. The switching (coupling, probe) field drives the transition  $|1\rangle \leftrightarrow |2\rangle$  ( $|3\rangle \leftrightarrow |2\rangle$ ,  $|3\rangle \leftrightarrow |4\rangle$ ) with a detuning  $\Delta_s$  ( $\Delta_c, \Delta_p$ ) in the absence of thermal motion. At room temperature, the inevitable random thermal motion of the  $j$ th atom moving with velocity  $v_j$  causes the “microscopic” Doppler shifts,  $k_s v_j$ ,  $k_c v_j$ , and  $k_p v_j$  in the corresponding atomic transitions, respectively. The strength of the nonlinearity is strongly dependent on the effective detunings, and thus the Doppler shifts. Thus, these frequency shifts change the optical nonlinearity in a way strongly dependent on the propagation direction of the probe field with respect to the switching and coupling fields, leading to the chiral XKerr nonlinearity. We assume that  $|k_s| = |k_c| = |k_p| = k$ . Both the switching and coupling laser beams are left-moving such that  $k_s v_j = k_c v_j$ . In the above arrangement, the backward-moving (forward-moving) probe field “sees” the same (opposite) Doppler shift as the switching and coupling ones. Under the two-photon resonance condition, i.e.  $\Delta_c = \Delta_s = \delta$ , and  $|\Omega_s| \ll |\Omega_c|$  leading to  $\rho_{11} \approx 1$ , we can solve the master equation with the perturbation approach [53–55] and obtain the total XKerr nonlinearity averaged over the velocity distribution as [56–60]

$$\chi_f = X_0 \int \frac{\gamma_{23}}{(i\Delta_p + \gamma_{43})} \left( \frac{1}{\zeta} + \frac{1}{\zeta^*} \right) N(v) dv, \quad (1)$$

for the forward-moving probe field, and

$$\chi_b = X_0 \int \frac{\gamma_{23}}{[i(\Delta_p + 2kv) + \gamma_{43}]} \left( \frac{1}{\zeta} + \frac{1}{\zeta^*} \right) N(v) dv, \quad (2)$$

in the backward-moving case, where  $X_0 = 3\pi c^2 \gamma_{43} / 8\omega_p^2 \Gamma_3 (\gamma_{21} + \gamma_{23})$ ,  $\zeta = i(\delta + kv) + (\gamma_{21} + \gamma_{23} + \Gamma_3) + |\Omega_c|^2 / 2\Gamma_3$ , and  $c$  is the vacuum light speed. The velocity distribution is conventionally taken to be Maxwellian, i.e.  $N(v) = N_a e^{-v^2/u^2} / \sqrt{\pi} u$ , where  $u$  is the room-mean-square atomic velocity, and  $ku \approx 2\pi \times 300$  MHz for Rb atoms at room temperature [61]. In our arrangement, the linear susceptibility of the probe light is vanishingly small and can be neglected because  $\rho_{33} \approx 0$ . Compared with the backward input case, where the Doppler broadening significantly reduces the total XKerr nonlinearity [see Eq. (2)], the Doppler shift “seen” by the forward-moving probe field is partly compensated [see Eq. (1)] and subsequently the nonlinearity remains large. This chirality is a combination of thermal motion and the unidirectionality of the switching and coupling lasers. The Doppler shift is due to the atomic thermal motion. The unidirectionally propagating switching and coupling lasers break the spatial symmetry, leading to a direction-dependent response to the probe laser. Without the switching and coupling fields, the thermal motion sharply suppresses the atomic susceptibility in both directions. If the control fields in EIT are applied to atoms from two opposite directions, thermal motion will be detrimental [39, 40]. In the two latter cases, the chirality disappears. Note that the reduced absorption in the “two-photon Doppler-free” configuration for EIT in a 3D atomic sample has been observed [62]. The two-port non-reciprocal transport has been experimentally demonstrated as a result of atomic thermal motion and the strong atom-cavity coupling [63]. However, cavity-free optical isolation exploiting thermal motion is conceptually different and admirable because its realization can be simpler and it can implement multiport optical circulators.

Unlike the configurations for quantum gates [51] and non-destructive detection of photons [64], the applied switching and coupling modes are [chosen here](#) to be much stronger than the probe laser beam. The backaction on the switching field due to the probe photon is negligible. Thus, they can be considered as constant in atoms. We apply the slowly-varying envelope approximation to the probe field. The backscattering is negligible during the propagation, and the probe photon propagates unidirectionally [51, 65]. When  $|\Omega_c| \gg |\Omega_s| \gg |\Omega_p|$ , the propagation of the probe pulse in atoms is described by Maxwell equations by taking into account the XKerr nonlinearity [66, 67]:

$$\frac{\partial \Omega_p^f(z, t)}{\partial z} + \frac{1}{c} \frac{\partial \Omega_p^f(z, t)}{\partial t} = -\chi_f |\Omega_s|^2 \Omega_p^f(z, t), \quad (3)$$

$$\frac{\partial \Omega_p^b(z', t)}{\partial z'} + \frac{1}{c} \frac{\partial \Omega_p^b(z', t)}{\partial t} = -\chi_b |\Omega_s|^2 \Omega_p^b(z', t), \quad (4)$$

for the forward- and backward-moving probe pulses, respectively, and  $z' = L - z$ . When  $\chi_f = \chi_b$  as in usual Kerr nonlinear

isolators, the medium is reciprocal for the probe beam. However, the medium can be non-reciprocal even for two weak counter-propagating probe beams co-existing in the medium simultaneously when  $\chi_f$  and  $\chi_b$  are very different. Therefore, optical isolators or circulators using this chiral medium can overcome the dynamical reciprocity in conventional nonlinear isolators [25]. We focus on the steady-state solution, where a long probe pulse is constant in time at position  $z$  [51], such that  $\frac{1}{c} \frac{\partial \Omega_p^j}{\partial t} \approx 0$  and  $\frac{1}{c} \frac{\partial \Omega_s^j}{\partial t} \approx 0$ . After passing through the atomic medium with length  $L$ , the probe fields become

$$\Omega_p^j(L) = \xi_j e^{i\phi_j} \Omega_p^j(0), \quad (5)$$

where  $\xi_j = \exp(-\text{Re}[\chi_j]|\Omega_s|^2 L)$  and  $\phi_j = -\text{Im}[\chi_j]|\Omega_s|^2 L$ , with  $j = f, b$ , are the corresponding transmission amplitude and phase shift, respectively. When  $|\Delta_p| \gg \gamma_{43}$  and  $|\Omega_c|^2/2\Gamma_3 \gg |\delta + kv|$ , to a good approximation, we have  $\phi_f \approx N_a L \frac{3\pi c^2}{4\omega_p^2} \frac{\gamma_0}{\Delta_p} \frac{|\Omega_s|^2}{|\Omega_c|^2}$  and  $\xi_f \approx \exp\left(-N_a L \frac{3\pi c^2}{4\omega_p^2} \frac{\gamma_0}{\Delta_p} \frac{|\Omega_s|^2}{|\Omega_c|^2}\right)$ . The transmission is calculated as  $|\xi_j|^2$ . In contrast, the transmission and phase modulation of the backward-moving probe laser are much smaller.

Obviously, an optical isolator can be realized when  $\xi_f \gg \xi_b$ . For  $\xi_f \approx \xi_b$  and  $\phi_f - \phi_b \approx \pi$ , an optical circulator could be made by inserting the atomic vapor in a MZI, as shown in Fig. 1(a). To achieve that, two beam splitters (BSs) are needed to first divide the input probe pulse into two paths and then mix them after passing through the nonlinear medium. The two BSs are chosen to be identical with reflection and transmission amplitudes of  $\sin \theta$  and  $\cos \theta$ , respectively. The relative phase in these amplitudes is  $\varphi$ . Their operation on photons is determined by  $H_{\text{BS}} = \theta e^{i\varphi} \hat{a}_{\text{in}}^\dagger \hat{b}_{\text{in}} + \theta e^{-i\varphi} \hat{a}_{\text{in}} \hat{b}_{\text{in}}^\dagger$  [68]. A fixed phase shift  $\vartheta$  in the lower path compensates the phase shift  $\phi_b$  of the backward-moving probe laser beam caused by the nonlinear medium. Therefore, the backward-moving probe photons entering the BS1 has the same phase in the upper and lower waveguides. Applying  $H_{\text{BS}}$  and the transmission relation Eq. 5, we obtain the forward transmission matrix elements between the input and output ports as

$$T_{12} = \left| \frac{a_o}{a_{\text{in}}} \right|^2 = \left| \xi_f e^{i(\phi_f - \vartheta)} \cos^2 \theta - \sin^2 \theta \right|^2, \quad (6a)$$

$$T_{32} = \left| \frac{a_o}{b_{\text{in}}} \right|^2 = \left| (1 + \xi_f e^{i(\phi_f - \vartheta)}) \cos \theta \sin \theta \right|^2, \quad (6b)$$

$$T_{14} = \left| \frac{b_o}{a_{\text{in}}} \right|^2 = \left| (1 + \xi_f e^{i(\phi_f - \vartheta)}) \cos \theta \sin \theta \right|^2, \quad (6c)$$

$$T_{34} = \left| \frac{b_o}{b_{\text{in}}} \right|^2 = \left| \cos^2 \theta - \xi_f e^{i(\phi_f - \vartheta)} \sin^2 \theta \right|^2, \quad (6d)$$

where  $T_{mn}$  is the transmission coefficient from port  $m$  to port  $n$ , with  $m, n = 1, 2, 3, 4$ . Exchanging the inputs and the outputs, and replacing  $\xi_f$  and  $\phi_f$  with  $\xi_b$  and  $\phi_b$  in  $T_{mn}$ , respectively, we obtain the transmission matrix element  $T_{nm}$  for the backward-moving case. Optical non-reciprocity requires  $T_{mn} \neq T_{nm}$  for  $m \neq n$ . We have  $T_{mm} = 0$  in the circulator. Also, the backscattering to ports at the same side as the input is negligible, so

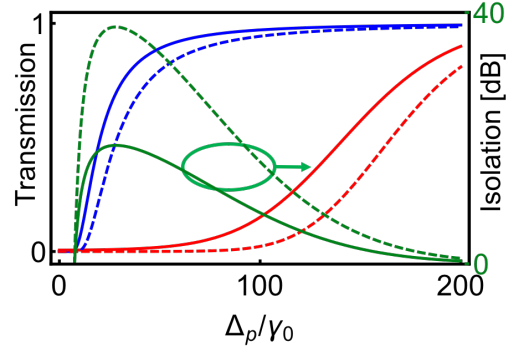


FIG. 2. (Color online) Transmission of an isolator for the right-moving (blue curves) and left-moving (red curves) probe fields, and isolation ratio (green curves associating with the right vertical axis) as a function of the probe detuning  $\Delta_p$ . Solid (dashed) curves are for  $L = 2$  (4) cm. Other parameters are  $N_a = 5 \times 10^{12} \text{ cm}^{-3}$ ,  $\Gamma_3 = 0.1\gamma_0$ ,  $\Omega_c = 20\gamma_0$ ,  $\Omega_s = 4\gamma_0$ , and  $\delta = 0$ .

that  $T_{31} = T_{13} = T_{41} = T_{14}$  (see details in the supplementary material). An ideal circulator, in which the photons flow along  $1 \rightarrow 2 \rightarrow 3 \rightarrow 4 \rightarrow 1$ , has a transmission matrix  $T^{\text{id}}$  with elements  $T_{12}^{\text{id}} = T_{23}^{\text{id}} = T_{34}^{\text{id}} = T_{41}^{\text{id}} = 1$  and others zero. Note that  $\text{Tr}[T^{\text{id}} \cdot T^{\text{id},T}] = 4$ .

Hereafter, we take  $\delta = 0$  and  $\omega_p/2\pi \sim 384 \text{ THz}$  for the  $D_1$  line of Rb atoms, and choose the parameters  $N_a = 5 \times 10^{12} \text{ cm}^{-3}$ ,  $\Gamma_3 = 0.1\gamma_0$ ,  $\Omega_c = 20\gamma_0$ , and  $\Omega_s = 4\gamma_0$ , yielding  $\rho_{11} \approx 0.96$ . Such large switching light can enhance the cross phase modulation of the probe field.

*Isolator.* — For a cm-scale medium, e.g.  $L = 2 \text{ cm}$ , the medium is absorptive. The forward and backward transmissions are very different, see Fig. 2. As the probe detuning increases, the forward transmission  $T_{12}$  rapidly increases to a high value of 0.80 at  $\Delta_p = 35.6\gamma_0$ , corresponding to an insertion loss of 1 dB. Due to Doppler broadening, the backward-moving probe field suffers a larger absorption. Therefore, the backward transmission  $T_{21}$  is much smaller than  $T_{12}$ , when  $35.6\gamma_0 < \Delta_p < 60.6\gamma_0$ . In this region, the insertion loss is smaller than 1 dB, while the isolation ratio is larger than 15 dB. The isolation ratio can be considerably improved with a large forward transmission by using a longer medium, or equivalently increasing the atomic density. The non-reciprocal window of frequency slightly moves to larger detuning. For  $L = 4 \text{ cm}$ , the isolation ratio can reach more than 30 dB in the range of  $50\gamma_0 < \Delta_p < 60\gamma_0$ , yielding an isolation bandwidth of  $2\pi \times 60 \text{ MHz}$ . At the same time, the insertion loss remains low, less than 1 dB. Thus, we can simply use this medium as an isolator.

*Circulator.* — For a short medium, the transmissions of the forward- and backward-moving probes can be comparably high. However, at a particular probe frequency, the phase shift difference between these two opposite propagating probes can approach  $\pi$ . As shown in Fig. 3(a), for  $L = 3.33 \text{ mm}$ , the phase shift  $\phi_b$  is always small, specifically about  $0.011\pi$  at  $\Delta_p = 7.77\gamma_0$ . In contrast,  $\phi_f$  exponentially decays from about  $2\pi$  at  $\Delta_p = 3.5\gamma_0$  to  $0.5\pi$  at  $\Delta_p = 15.5\gamma_0$ . At the optimal point

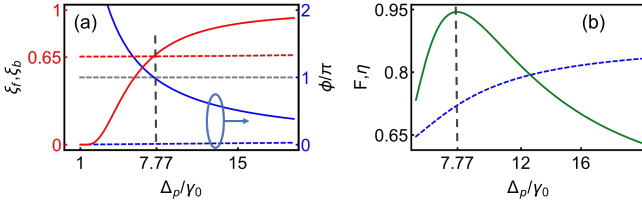


FIG. 3. (Color online) Circulator performance versus the detuning  $\Delta_p$ . (a) Phase shifts (blue curves) and transmission amplitudes (red curves) for right- (solid curves) and left-moving (dashed lines) probe fields as a function of the probe detuning  $\Delta_p$ . (b) Fidelity (green curves) and average insertion loss (blue dashed curves) of an optical circulator as a function of  $\Delta_p$ . The vertical black dashed lines in the two figures show the optimal detuning  $\Delta_p^{\text{opt}}/\gamma_0 = 7.77$  when  $\phi_f^{\text{opt}} - \phi_b^{\text{opt}} = \pi$  and  $\xi_f^{\text{opt}} \approx \xi_b^{\text{opt}} \approx 0.66$ . The length of the atomic medium is 3.33 mm. Other parameters are as in Fig. 2.

$\Delta_p^{\text{opt}} = 7.77\gamma_0$ , the difference of phase shifts,  $\phi_f - \phi_b$ , reaches the optimal value of  $\pi$ . At this point,  $\xi_f^{\text{opt}} \approx \xi_b^{\text{opt}} \approx 0.66$ . Thus, a high-performance circulator can be made by inserting this nonlinear medium into a MZI composed of unbalanced BSs. Here, we set  $\vartheta = 0.01\pi$  and  $\sin^2 \theta = 0.4 \approx \bar{\xi}/(1 + \bar{\xi})$  with  $\bar{\xi} = (\xi_f^{\text{opt}} + \xi_b^{\text{opt}})/2$ .

The performance of a circulator can be quantified with the fidelity  $\mathcal{F}$  and the average photon survival probability  $\eta$  [43]. The fidelity is evaluated as the overlap of the renormalized transmission matrix  $\tilde{T} = (T_{ij}/\eta_i)$ , with the ideal one,  $T^{\text{id}}$ . Here,  $\eta_i = \sum_k T_{i,k}$  is the survival probability of the probe photons entering port  $i$ . The average operation fidelity of the circulator is then  $\mathcal{F} = \text{Tr}[\tilde{T} \cdot T^{\text{id},T}]/\text{Tr}[T^{\text{id}} \cdot T^{\text{id},T}]$ , giving the probability of a correct circulator operation averaged over various inputs. The minimum fidelity is  $\mathcal{F} = 0$ , while an ideal operation yields  $\mathcal{F} = 1$ . The average photon survival probability  $\eta = \sum_i \eta_i/4$  is another important figure characterizing the four-port circulator. We scan the probe frequency to find the working window of the circulator in Fig. 3. As the detuning  $\Delta_p$  varies from  $6\gamma_0$  to  $20\gamma_0$ , the fidelity first rises up rapidly and reaches the maximum 0.944 at  $\Delta_p^{\text{opt}} = 7.77\gamma_0$ , then decreases to a small value of 0.63. During this sweep,  $\eta$  increases from 0.68 to about 0.83. Although the photons have a larger probability to survive at a large detuning, the fidelity is low. As a trade-off, the circulator operating within the frequency range  $6.6\gamma_0 < \Delta_p < 9.7\gamma_0$  can achieve a fidelity larger than 0.9 at the expense of  $\eta > 0.69$ . The corresponding working window is about  $2\pi \times 20$  MHz and the average insertion loss is about 1.6 dB. If  $\vartheta = 0$ , the fidelity and insertion loss only reduce very slightly.

At  $\Delta_p^{\text{opt}}$ , we obtain  $\mathcal{F} = 0.944$  and  $\eta = 0.72$ , yielding an insertion loss of 1.42 dB. The corresponding transmission matrix is shown in Fig. 4. The obtained matrix is close to that of the ideal circulator, implying that a good optical non-reciprocity is obtained. We can also quantify the circulator performance by the isolations,  $I_i = -10 \log(T_{i+1,i}/T_{i,i+1})$ , of the four optical isolators formed between adjacent ports [43] and have  $\{I_i\} = \{41.7, 13.8, 13.8, 8.2\}$  dB with  $i = \{1, 2, 3, 4\}$ ,

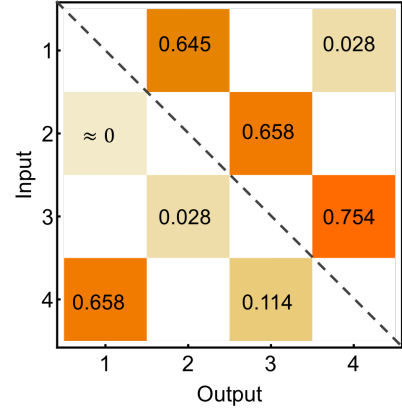


FIG. 4. (Color online) Transmission matrix of an optical circulator at the optimal point,  $\Delta_p^{\text{opt}}/\gamma_0 = 7.77$ . The numbers inside the color squares are the transmission between the two ports. The transmissions in white areas are zero. Other parameters are as in Fig. 3.

implying non-reciprocal photon circulation along  $1 \rightarrow 2 \rightarrow 3 \rightarrow 4 \rightarrow 1$ . The achieved performance is already useful for practical optical isolation [43].

*Implementation.* — The required 1D nonlinear waveguide embedded with alkali atoms can be made with various methods and platforms [42, 46–50, 69–74]. A feasible platform can be a cm-scale hollow-core photonic crystal fiber filled with Rb atoms at room temperature [49, 74]. A few-photon-level memory and a strong XKerr nonlinearity have been demonstrated with a weak control field in such platform [49, 74]. For an on-chip realization, we consider a zigzag waveguide clad with high-density Rb atoms, allowing a coherent light-atom interaction [71–73]. To conduct a N-type configuration, we couple the lasers to the  $D_1$  lines of the Rb atom, yielding  $\omega_p/2\pi \sim 384$  THz. A linearly-polarized probe field drives the transition  $|5^2S_{1/2}, F = 2, m_s = 0\rangle \leftrightarrow |5^2P_{1/2}, F' = 2, m'_s = 0\rangle$ . The linearly-polarized switching light couples to  $|5^2S_{1/2}, F = 1, m_s = -1\rangle \leftrightarrow |5^2P_{1/2}, F' = 1, m'_s = -1\rangle$ . The strong left-circularly-polarized coupling field is applied between  $|5^2S_{1/2}, F = 2, m_s = 0\rangle \leftrightarrow |5^2P_{1/2}, F' = 1, m'_s = -1\rangle$ . Thus, the optical isolation can be performed for a linearly-polarized light.

*Conclusion.* — We have presented new ways to realize optical isolators and circulators using chiral XKerr nonlinearity of N-type atoms embedded in a 1D waveguide. The four-port optical circulator can reach a high fidelity of 0.9 and a small insertion loss of 1.6 dB. Our proposal may provide a new vision for nonlinear optical isolation without dynamic reciprocity because the XKerr nonlinearity itself is chiral, and the isolation is based on the linear Eqs. 3 and 4. A large XKerr nonlinearity has been reported at the single-photon level [49, 51]. Therefore, our method can be extended to the quantum regime, realizing an optical circulator for a single-photon probe on a chip at room temperature.

We acknowledge Dr. Sahin Ozdemir for helpful discussions. K.X. and M.X. would like to thank the support of the National Key R&D Program of China (Grant No.

2017YFA0303703), and the National Natural and Science Foundation of China (Grant Nos. 11874212 and 61435007). F.N. is supported in part by the MURI Center for Dynamic Magneto-Optics via the Air Force Office of Scientific Research (AFOSR) (FA9550-14-1-0040), Army Research Office (ARO) (Grant No. 73315PH), Asian Office of Aerospace Research and Development (AOARD) (Grant No. FA2386-18-1-4045), Japan Science and Technology Agency (JST) (the IMPACT program and CREST Grant No. JPMJCR1676), Japan Society for the Promotion of Science (JSPS) (JSPS-RFBR Grant No. 17-52-50023, JSPS-FWO Grant No. VS.059.18N), RIKEN-AIST Challenge Research Fund, and the John Templeton Foundation.

---

\* keyu.xia@nju.edu.cn

- [1] J. I. Cirac, P. Zoller, H. J. Kimble, and H. Mabuchi, “Quantum state transfer and entanglement distribution among distant nodes in a quantum network,” *Phys. Rev. Lett.* **78**, 3221–3224 (1997).
- [2] H. J. Kimble, “The quantum internet,” *Nature* **453**, 1023–1030 (2008).
- [3] D. Jalas, A. Petrov, M. Eich, W. Freude, S. Fan, Z. Yu, R. Baets, M. Popović, A. Melloni, J. D. Joannopoulos, M. Vanwolleghem, C. R. Doerr, and H. Renner, “What is –and what is not –an optical isolator,” *Nat. Photon.* **7**, 579–582 (2013).
- [4] Z. Yu and S. Fan, “Optical isolation based on nonreciprocal phase shift induced by interband photonic transitions,” *Appl. Phys. Lett.* **94**, 171116 (2009).
- [5] D. L. Sounas and A. Alù, “Non-reciprocal photonics based on time modulation,” *Nat. Photon.* **11**, 774–783 (2017).
- [6] Z. Yu and S. Fan, “Complete optical isolation created by indirect interband photonic transitions,” *Nat. Photon.* **3**, 91–94 (2009).
- [7] M. S. Kang, A. Butsch, and P. St. J. Russell, “Reconfigurable light-driven opto-acoustic isolators in photonic crystal fibre,” *Nat. Photon.* **5**, 549–553 (2011).
- [8] K. Fang, Z. Yu, and S. Fan, “Realizing effective magnetic field for photons by controlling the phase of dynamic modulation,” *Nat. Photon.* **6**, 782–787 (2012).
- [9] K. Fang, Z. Yu, and S. Fan, “Photonic Aharonov-Bohm effect based on dynamic modulation,” *Phys. Rev. Lett.* **108**, 153901 (2012).
- [10] K. Fang, J. Luo, A. Metelmann, M. H. Matheny, F. Marquardt, A. A. Clerk, and O. Painter, “Generalized non-reciprocity in an optomechanical circuit via synthetic magnetism and reservoir engineering,” *Nat. Phys.* **13**, 465–471 (2017).
- [11] L. D. Tzuan, K. Fang, P. Nussenzveig, S. Fan, and M. Lipson, “Non-reciprocal phase shift induced by an effective magnetic flux for light,” *Nat. Photon.* **8**, 701–705 (2014).
- [12] N. Jia, N. Schine, A. Georgakopoulos, A. Ryou, A. Sommer, and J. Simon, “Photons and polaritons in a broken-time-reversal nonplanar resonator,” *Phys. Rev. A* **97**, 013802 (2018).
- [13] S. Maayani, R. Dahan, Y. Kligerman, E. Moses, A. U. Hassan, H. Jing, F. Nori, D. N. Christodoulides, and T. Carmon, “Flying couplers above spinning resonators generate irreversible refraction,” *Nature* **558**, 569–572 (2018).
- [14] M. Hafezi and P. Rabl, “Optomechanically induced non-reciprocity in microring resonators,” *Opt. Express* **20**, 7672–7684 (2012).
- [15] Z. Shen, Y.-L. Zhang, Y. Chen, C.-L. Zou, Y.-F. Xiao, X.-B. Zou, F.-W. Sun, G.-C. Guo, and C.-H. Dong, “Experimental realization of optomechanically induced non-reciprocity,” *Nat. Photon.* **10**, 657–662 (2016).
- [16] F. Ruesink, M.-A. Miri, A. Alù, and E. Verhagen, “Nonreciprocity and magnetic-free isolation based on optomechanical interactions,” *Nat. Commun.* **7**, 13662 (2016).
- [17] M. Soljačić, C. Luo, J. D. Joannopoulos, and S. Fan, “Nonlinear photonic crystal microdevices for optical integration,” *Opt. Lett.* **28**, 637–639 (2003).
- [18] L. Fan, J. Wang, L. T. Varghese, H. Shen, B. Niu, Y. Xuan, A. M. Weiner, and M. Qi, “An all-silicon passive optical diode,” *Science* **335**, 447–450 (2012).
- [19] L. Chang, X. Jiang, S. Hua, C. Yang, J. Wen, L. Jiang, G. Li, G. Wang, and M. Xiao, “Parity-time symmetry and variable optical isolation in active-passive-coupled microresonators,” *Nat. Photon.* **8**, 524–529 (2014).
- [20] B. Peng, Ş. K. Özdemir, F. Lei, F. Monifi, M. Gianfreda, G. L. Long, S. Fan, F. Nori, C. M. Bender, and L. Yang, “Parity-time-symmetric Whispering-Gallery microcavities,” *Nat. Phys.* **10**, 394–398 (2014).
- [21] N. Bender, S. Factor, J. D. Bodyfelt, H. Ramezani, D. N. Christodoulides, F. M. Ellis, and T. Kottos, “Observation of asymmetric transport in structures with active nonlinearities,” *Phys. Rev. Lett.* **110**, 234101 (2013).
- [22] S. Hua, J. Wen, X. Jiang, Q. Hua, L. Jiang, and M. Xiao, “Demonstration of a chip-based optical isolator with parametric amplification,” *Nat. Commun.* **7**, 13657 (2016).
- [23] Y. Zheng, J. Yang, Z. Shen, J. Cao, X. Chen, X. Liang, and W. Wan, “Optically induced transparency in a micro-cavity,” *Light: Science & Applications* **5**, e16072 (2016).
- [24] B. He, L. Yang, X. Jiang, and M. Xiao, “Transmission non-reciprocity in a mutually coupled circulating structure,” *Phys. Rev. Lett.* **120**, 203904 (2018).
- [25] Y. Shi, Z. Yu, and S. Fan, “Limitations of nonlinear optical isolators due to dynamic reciprocity,” *Nat. Photon.* **9**, 388–392 (2015).
- [26] A. B. Khanikaev and A. Alù, “Nonlinear dynamic reciprocity,” *Nat. Photon.* **9**, 359–361 (2015).
- [27] B. Peng, Ş. K. Özdemir, W. Chen, F. Nori, and L. Yang, “What is and what is not electromagnetically induced transparency in Whispering-Gallery microcavities,” *Nat. Commun.* **5**, 5082 (2014).
- [28] H.-C. Sun, Y.-x. Liu, H. Ian, J. Q. You, E. Il’ichev, and Franco Nori, “Electromagnetically induced transparency and Autler-Townes splitting in superconducting flux quantum circuits,” *Phys. Rev. A* **89**, 063822 (2014).
- [29] H. Ian, Y.-x. Liu, and F. Nori, “Tunable electromagnetically induced transparency and absorption with dressed superconducting qubits,” *Phys. Rev. A* **81**, 063823 (2010).
- [30] P. Lodahl, S. Mahmoodian, S. Stobbe, A. Rauschenbeutel, P. Schneeweiss, J. Volz, H. Pichler, and P. Zoller, “Chiral quantum optics,” *Nature* **541**, 473–480 (2017).
- [31] C. Y. Hu, “Spin-based single-photon transistor, dynamic random access memory, diodes, and routers in semiconductors,” *Phys. Rev. B* **94**, 245307 (2016).
- [32] R. Huang, A. Miranowicz, J. -Q. Liao, F. Nori, and H. Jing, “Nonreciprocal photon blockade,” *Phys. Rev. Lett.* **121**, 153601 (2018).
- [33] Y. Tang and A. E. Cohen, “Optical chirality and its interaction with matter,” *Phys. Rev. Lett.* **104**, 163901 (2010).
- [34] K. Y. Bliokh, D. Smirnova, and F. Nori, “Quantum spin Hall effect of light,” *Science* **348**, 1448–1451 (2015).
- [35] K. Y. Bliokh, F. J. Rodríguez-Fortuño, F. Nori, and A. V. Zay-

- ats, “Spin-orbit interactions of light,” *Nat. Photon.* **9**, 796–808 (2015).
- [36] K. Y. Bliokh and F. Nori, “Transverse and longitudinal angular momenta of light,” *Phys. Rep.* **592**, 1–38 (2015).
- [37] K. Y. Bliokh and F. Nori, “Characterizing optical chirality,” *Phys. Rev. A* **83**, 021803(R) (2011).
- [38] T. Li, A. Miranowicz, X. Hu, K. Xia, and F. Nori, “Quantum memory and gates using a  $\Lambda$ -type quantum emitter coupled to a chiral waveguide,” *Phys. Rev. A* **97**, 062318 (2018).
- [39] D.-W. Wang, H.-T. Zhou, M.-J. Guo, J.-X. Zhang, J. Evers, and S.-Y. Zhu, “Optical diode made from a moving photonic crystal,” *Phys. Rev. Lett.* **110**, 093901 (2013).
- [40] S. A. R. Horsley, J.-H. Wu, M. Artoni, and G. C. La Rocca, “Optical nonreciprocity of cold atom Bragg mirrors in motion,” *Phys. Rev. Lett.* **110**, 223602 (2013).
- [41] H. Ramezani, P. K. Jha, Y. Wang, and X. Zhang, “Nonreciprocal localization of photons,” *Phys. Rev. Lett.* **120**, 043901 (2018).
- [42] C. Sayrin, C. Junge, R. Mitsch, B. Albrecht, D. O’Shea, P. Schneeweiss, J. Volz, and A. Rauschenbeutel, “Nanophotonic optical isolator controlled by the internal state of cold atoms,” *Phys. Rev. X* **5**, 041036 (2015).
- [43] M. Scheucher, A. Hilico, E. Will, J. Volz, and A. Rauschenbeutel, “Quantum optical circulator controlled by a single chirally coupled atom,” *Science* **354**, 1577–1580 (2016).
- [44] I. Söllner, S. Mahmoodian, S. L. Hansen, L. Midolo, A. Javadi, G. Kiršanskė, T. Pregnolato, H. El-Ella, E. H. Lee, J. D. Song, S. Stobbe, and P. Lodahl, “Deterministic photon-emitter coupling in chiral photonic circuits,” *Nat. Nanotech.* **10**, 775–778 (2015).
- [45] K. Xia, G. Lu, G. Lin, Y. Cheng, Y. Niu, S. Gong, and J. Twamley, “Reversible nonmagnetic single-photon isolation using unbalanced quantum coupling,” *Phys. Rev. A* **90**, 043802 (2014).
- [46] H. Schmidt and A. R. Hawkins, “Electromagnetically induced transparency in alkali atoms intergrated on a semiconductor chip,” *Appl. Phys. Lett.* **86**, 032106 (2005).
- [47] E. J. Lunt, B. Wu, J. M. Keeley, P. Measor, H. Schmidt, and A. R. Hawkins, “Hollow ARROW waveguides on self-aligned pedestals for improved geometry and transmission,” *IEEE Photon. Technol. Lett.* **22**, 1147–1149 (2010).
- [48] L. Stern, B. Desiatov, I. Goykhman, and U. Levy, “Nanoscale light-matter interactions in atomic cladding waveguides,” *Nat. Commun.* **4**, 1548 (2013).
- [49] V. Venkataraman, K. Saha, and A. L. Gaeta, “Phase modulation at the few-photon level for weak-nonlinearity-based quantum computing,” *Nat. Photon.* **7**, 138–141 (2012).
- [50] G. Epple, K. S. Kleinbach, T. G. Euser, N. Y. Joly, T. Pfau, P. St. J. Russell, and R. Löw, “Rydberg atoms in hollow-core photonic crystal fibres,” *Nat. Commun.* **5**, 4132 (2014).
- [51] Z.-Y. Liu, Y.-H. Chen, Y.-C. Chen, H.-Y. Lo, P.-J. Tsai, I. A. Yu, Y.-C. Chen, and Y.-F. Chen, “Large cross-phase modulation at the few-photon level,” *Phys. Rev. Lett.* **117**, 203601 (2016).
- [52] H. Schmidt and A. Imamoglu, “Giant Kerr nonlinearities obtained by electromagnetically induced transparency,” *Opt. Lett.* **21**, 1936–1938 (1996).
- [53] R. W. Boyd, *Nonlinear Optics*, 3rd ed. (Elsevier, 2008).
- [54] Y. Q. Li and M. Xiao, “Electromagnetically induced transparency in a three-level  $\Lambda$ -type system in rubidium atoms,” *Phys. Rev. A* **51**, R2703 (1995).
- [55] J. Sheng, X. Yang, H. Wu, and M. Xiao, “Modified self-Kerr nonlinearity in a four-level N-type atomic system,” *Phys. Rev. A* **84**, 053820 (2011).
- [56] See Supplemental Material for the derivation of the cross-Kerr nonlinearity, which includes Refs. [57–60].
- [57] K. Xia, M. Alamri, and M. Suhail Zubairy, “Ultrabroadband nonreciprocal transverse energy flow of light in linear passive photonic circuits,” *Opt. Express* **21**, 25619–25631 (2013).
- [58] K. Okamoto, *Fundamental of Optics Waveguides*, 2nd ed. (Elsevier, 2006).
- [59] H. Wang, D. J. Goorskey, and M. Xiao, “Atomic coherence induced Kerr nonlinearity enhancement in Rb vapour,” *J. Mod. Opt.* **49**, 335–347 (2002).
- [60] M. O. Scully, and M. Suhail Zubairy, *Quantum Optics*, (Cambridge University, 1997).
- [61] H. Wu, J. Gea-Banacloche, and M. Xiao, “Observation of intracavity electromagnetically induced transparency and polariton resonances in a Doppler-broadened medium,” *Phys. Rev. Lett.* **100**, 173602 (2008).
- [62] J. Gea-Banacloche, Y.-Q. Li, S.-Z. Jin, and M. Xiao, “Electromagnetically induced transparency in ladder-type inhomogeneously broadened media: Theory and experiment,” *Phys. Rev. A* **51**, 576–584 (1995).
- [63] S. Zhang, Y. Hu, G. Lin, Y. Niu, K. Xia, J. Gong, and S. Gong, “Thermal-motion-induced non-reciprocal quantum optical system,” *Nat. Photon.* 10.1038/s41566-018-0269-2 (2018).
- [64] K. Xia, M. Johnsson, P. L. Knight, and J. Twamley, “Cavity-free scheme for nondestructive detection of a single optical photon,” *Phys. Rev. Lett.* **116**, 023601 (2016).
- [65] M. Fleischhauer, A. Imamoglu, and J. P. Marangos, “Electromagnetically induced transparency: Optics in coherent media,” *Rev. Mod. Phys.* **77**, 633–673 (2005).
- [66] See Supplemental Material for the propagation equation of the field in an 1D space, which includes Refs. [67].
- [67] K. Xia, S. Q. Gong, C. Liu, X. Song, and Y. Niu, “Near dipole-dipole effects on the propagation of few-cycle pulse in a dense two-level medium,” *Opt. Express* **13**, 5913–5924 (2005).
- [68] P. Kok, W. J. Munro, K. Nemoto, T. C. Ralph, J. P. Dowling, and G. J. Milburn, “Linear optical quantum computing with photonic qubits,” *Rev. Mod. Phys.* **79**, 135–174 (2007).
- [69] F. Le Kien and A. Rauschenbeutel, “Electromagnetically induced transparency for guided light in an atomic array outside an optical nanofiber,” *Phys. Rev. A* **91**, 053847 (2015).
- [70] T. Nieddu, V. Gokhroo, and S. N. Chormaic, “Optical nanofibres and neutral atoms,” *J. Opt.* **18**, 053001 (2016).
- [71] L. Stern, B. Desiatov, N. Mazurski, and U. Levy, “Strong coupling and high-contrast all-optical modulation in atomic cladding waveguides,” *Nat. Commun.* **8**, 14461 (2016).
- [72] R. Ritter, N. Gruhler, H. Dobbertin, H. Kübler, S. Scheel, W. Pernice, T. Pfau, and R. Löw, “Coupling thermal atomic vapor to slot waveguides,” *Phys. Rev. X* **8**, 021032 (2018).
- [73] R. Ritter, N. Gruhler, W. Pernice, H. Kübler, T. Pfau, and R. Löw, “Atomic vapor spectroscopy in integrated photonic structures,” *Appl. Phys. Lett.* **107**, 041101 (2015).
- [74] M. R. Sprague, P. S. Michelberger, T. F. M. Champion, D. G. England, J. Nunn, X.-M. Jin, W. S. Kolthammer, A. Abdolvand, P. St. J. Russell, and I. A. Walmsley, “Broadband single-photon-level memory in a hollow-core photonic crystal fibre,” *Nat. Photon.* **8**, 287–291 (2014).